J. Am. Soc. Mass Spectrom. (2011) 22:762–772
DOI: 10.1007/s13361-010-0066-8

RESEARCH ARTICLE

Analysis of Amphiphilic Lipids and Hydrophobic Proteins Using Nonresonant Femtosecond Laser Vaporization with Electrospray Post-Ionization

John J. Brady, Elizabeth J. Judge, Robert J. Levis

Center for Advanced Photonics Research, Department of Chemistry, Temple University, 1901 N 13th Street, Philadelphia, PA 19122, USA

Abstract

Amphiphilic lipids and hydrophobic proteins are vaporized at atmospheric pressure using nonresonant 70 femtosecond (fs) laser pulses followed by electrospray post-ionization prior to being transferred into a time-of-flight mass spectrometer for mass analysis. Measurements of molecules on metal and transparent dielectric surfaces indicate that vaporization occurs through a nonthermal mechanism. The molecules analyzed include the lipids 1-monooleoyl-rac-glycerol, 1,2-dihexanoyl-*sn*-glycero-3-phosphocholine, 1,2-dimyristoyl-*sn*-glycero-3-phosphocholine, and the hydrophobic proteins gramicidin A, B, and C. Vaporization of lipids from blood and milk are also presented to demonstrate that lipids in complex systems can be transferred intact into the gas phase for mass analysis.

Key words: Femtosecond, Electrospray, Lipids, Vaporization, Laser, Atmospheric, Nonresonant

Introduction

Amphiphilic and hydrophobic molecules play important parts in biology; for example, glycerolipids, sphingolipids, and sterol lipids are central to membrane formation, energy storage, signaling, and metabolism. Mass spectrometry is playing an increasing role in lipid detection as indicated by electrospray ionization (ESI) [1], matrix-assisted laser desorption ionization (MALDI) [2], fast atom bombardment (FAB) [3], and secondary ion mass spectrometry (SIMS) [4]. Although these techniques have been successful in detecting lipids, there are several drawbacks to the current analysis methods from a systems biology point of view. For conventional ESI-MS analysis, a tissue sample must be homogenized prior to extraction of the amphiphilic lipids and proteins, causing a loss of spatial distribution information. Laser and particle-based techniques, such as MALDI, FAB, and SIMS, overcome this problem by analyzing the tissue directly. However, laser and particle-based techniques are typically performed under vacuum, deleteriously altering the biological system through both sample preparation (microtome and freeze fracture) and low pressure conditions.

New techniques have been developed to relax sample preparation requirements and allow for *ex vivo* analysis at atmospheric pressure. Two-dimensional desorption electrospray ionization images of carcinogenic tissue revealed a difference in the lipid profile of normal, benign, and carcinogenic tissue [5–7]. The detection of lipids using laser-based techniques leads to enhanced spatial resolution in the analysis of tissue sections since the spatial resolution is determined by the diameter of the focused laser. Several nanosecond (ns) laser-based methods have been developed to transfer molecules from the condensed phase into the gas phase for atmospheric pressure ionization. Lipids from various samples have been analyzed using electrospray-assisted laser desorption ionization (ELDI) [8], matrix-assisted laser desorption electrospray ionization [9], and laser ablation electrospray ionization (LAESI) [10, 11].

Electronic supplementary material The online version of this article (doi:10.1007/s13361-010-0066-8) contains supplementary material, which is available to authorized users.

Correspondence to: Robert J. Levis; *e-mail:* rjlevis@temple.edu

Received: 21 October 2010
Revised: 17 December 2010
Accepted: 23 December 2010
Published online: 8 February 2011

Although these methods have successfully analyzed a variety of tissue samples and molecules, ns laser desorption causes rapid heating of the metal substrate at high intensities ($>10^8$ W/cm^2) leading to thermal desorption [12]. At lower intensities, the inherent water present in the tissue [9–11, 13–15], or addition of a small organic acid [9, 16] is required to enable desorption via a resonant excitation.

The ultrashort duration of the femtosecond (fs) laser pulse enables new coupling mechanisms in comparison with a ns duration laser pulse. Unlike the thermal mechanism present in ns laser desorption experiments, the energy from a fs laser pulse is deposited into the system (substrate and analyte) before the system can thermally respond [17]. This suggests that a fs laser pulse will allow the transfer of analyte into the gas phase without undergoing the decomposition anticipated if thermal equilibrium was obtained. Nonresonant fs laser pulses have been used previously to transfer material into the gas phase, typically under vacuum conditions, for mass analysis. The use of nonresonant fs laser pulses to vaporize material followed by electrospray post-ionization enables mass analysis of high molecular weight compounds. This method has been used for the analysis and detection of a dipeptide [18], pharmaceuticals [19], and explosives [20] in the technique known as laser electrospray mass spectroscopy (LEMS). Nonresonant fs excitation should, in principle, couple into and vaporize all molecules, implying that sample preparation (elution, mixing with matrix, and choosing samples with a particular electronic or vibrational transition) is not necessary. LEMS has been used to vaporize, ionize and analyze molecules without any preprocessing procedures.

The previous LEMS investigations demonstrated the ability to vaporize a wide variety of molecules using laser intensities on the order of 10^{13} W/cm^2, but provided little insight into the vaporization mechanism. Here we probe the mechanism of nonresonant fs laser vaporization while investigating the vaporization of amphiphilic lipids and hydrophobic proteins adsorbed on metal and dielectric surfaces. We investigate the lipids 1-monooleoyl-rac-glycerol, 1,2-dihexanoyl-*sn*-glycero-3-phosphocholine (DHPC), 1,2-dimyristoyl-*sn*-glycero-3-phosphocholine (DMPC), and the hydrophobic proteins gramicidin A, B, and C. The vaporization, ionization and analysis of lipids from biological fluids including blood and milk are also investigated to determine the ability to analyze complex mixtures using nonresonant fs laser vaporization.

Methods

Materials

The solid lipid samples of 1-monooleoyl-rac-glycerol, DHPC, and DMPC were purchased from MP Biomedicals (Solon, OH, USA), Avanti Polar Lipids, Inc. (Alabaster, AL, USA) and Avanti Polar Lipids, respectively. The solid hydrophobic protein mixture of gramicidin A, B, and C isolated from *Bacillus aneurinolyticus* (*Bacillus brevis*) was purchased from Sigma Aldrich (St. Louis, MO, USA). The gramicidin mixture contains 80%, 6%, and 14% of gramicidin A, B, and C, respectively [21]. The specific type of gramicidin is determined by the 11th amino acid in the 15 amino acid sequence. For example, gramicidin A has the sequence [22, 23] HCO-L-Val-Gly-L-Ala-D-Leu-L-Ala-D-Val-L-Val-D-Val-L-Trp-D-Leu-**L-Trp**-D-Leu-L-Trp-D-Leu-L-Trp-NH$(CH_2)_2$OH (mass = 1881 Da) while gramicidin B has the sequence HCO-L-Val-Gly-L-Ala-D-Leu-L-Ala-D-Val-L-Val-D-Val-L-Trp-D-Leu-**L-Phe**-D-Leu-L-Trp-D-Leu-L-Trp-NH$(CH_2)_2$OH (mass = 1842 Da). Gramicidin C (mass = 1858 Da) has the sequence HCO-L-Val-Gly-L-Ala-D-Leu-L-Ala-D-Val-L-Val-D-Val-L-Trp-D-Leu-**L-Tyr**-D-Leu-L-Trp-D-Leu-L-Trp-NH$(CH_2)_2$OH. Undiluted human blood was obtained from a healthy volunteer in accordance with University policy and procedure. The reduced fat and whole milk was purchased from a local market. All samples were used without purification.

Sample Preparation

The lipid and protein samples were diluted to 1×10^{-4} M in methanol (Fisher Scientific, Fair Lawn, NJ, USA). A 30 μL aliquot of each solution was deposited on separate stainless steel or transparent dielectric (glass) slides and allowed to air dry prior to analysis. Undiluted whole blood (20 μL) was deposited directly onto a stainless steel slide. A 2 μL aliquot of 10^{-3} M DHPC was added to the undiluted whole blood and mixed 60 s prior to analysis while in the aqueous state. One minute prior to LEMS analysis, a 300 μL aliquot of milk was deposited into a welled (45 mm×6 mm×1 mm) aluminum sample plate to deter evaporation. No further sample preparation was performed on the milk samples or the undiluted whole blood/DHPC mixture other than transfer to the sample plate. The metal or glass substrate was supported by a three-dimensional translation stage, which permitted the analysis of fresh sample.

UV/VIS Spectroscopy

The 1-monooleoyl-rac-glycerol and gramicidin samples were diluted to 1×10^{-6} M in methanol and characterized using a Jasco V-530 UV-VIS spectrometer in the wavelength range of 200 to 800 nm, with a resolution of 1 nm.

Mass Spectrometry

The mass spectrometer used in these experiments has been described previously [18–20]. Briefly, a custom built electrospray source was employed for ionizing and transferring the sample into a vacuum chamber where pulsed deflection orthogonal time-of-flight analysis (TOF) was performed. The electrospray source employs a grounded needle, a dielectric capillary (both ends coated with metal) biased to –5 kV, a skimmer and a hexapole operated in the trapping mode, where the positive ions are collected at 10 Hz. After exiting the ESI source, the ions are transferred

to the extraction region by a second hexapole where they are injected orthogonally into the linear TOF analyzer via two high voltage pulsers (Directed Energy Inc., Fort Collins, CO, USA and Quantum Technology Inc., Lake Mary, FL, USA) triggered 220 μs after the ions exit the first hexapole (270 μs for the protein experiments). The positive ions were then detected and the resulting mass spectra were averaged for 50 laser shots (5 s) using a digital oscilloscope.

Laser Vaporization and Ionization

A Ti:Sapphire oscillator seeded a regenerative amplifier to create a 2.5 mJ pulse centered at 800 nm with a pulse duration of 70 fs. The 1 kHz repetition rate of the laser was reduced to 10 Hz to couple to the electrospray system. The laser energy was reduced to 400 μJ/pulse using a neutral density filter for the experiments concerning vaporization from a metal substrate. An energy of 1 mJ/pulse was used to induce vaporization of sample from the glass substrate. The laser was focused to a spot size of ~250 μm in diameter using a 17.5 cm focal length lens, with an incident angle of 45° with respect to the sample. The intensity of the laser at the substrate was approximately 10^{13} W/cm^2. The area sampled was positioned ~6 mm below the ESI needle and 1 mm in front of the ESI needle. The vaporized plume was positioned along the axis of the ESI needle and inlet capillary. A schematic of the laser vaporization region is shown in the Supporting Information (SP1). The vaporized sample was captured and ionized by an electrospray plume composed of 1:1 (vol:vol) methanol:water acidified with 1.0% glacial acetic acid traveling perpendicular to the laser-vaporized material. In the nonpolar gramicidin experiments, the electrospray plume was composed of 80:20 (vol:vol) methanol:water acidified with 1.0% glacial acetic acid. The charged droplets were dried by counter propagating nitrogen gas before entering the inlet capillary.

Limit of Detection

The limit of detection (LOD) for the molecule DHPC was determined through comparison of LEMS and conventional ESI-MS data. The LEMS data was acquired by vaporizing the dried lipid, DHPC, from a metal slide after deposition of a 30 μL aliquot of a solution with varying molarity (1×10^{-4} to 5×10^{-6} M). The vaporized sample was captured and ionized by an electrospray plume composed of 1:1 (vol:vol) methanol:water acidified with 1.0% glacial acetic acid. Routinely, five averaged mass spectra, consisting of 50 laser shots each, could be acquired per sample. Conventional ESI-MS data was acquired by electrospraying a DHPC solution of varying sample molarity (5×10^{-6} to 5×10^{-8} M) dissolved in 1:1 (vol:vol) methanol:water acidified with 1.0% glacial acetic acid. Ten mass spectra, at each concentration investigated, were collected for the LEMS and conventional ESI-MS measurements.

Safety Consideration

Appropriate laser eye protection was worn by all personnel and the high voltage area was enclosed in plexiglass to prevent accidental contact with the biased electrodes. An exposure control plan was approved by the University for the blood analysis under protocol number 13314 in accordance with the policy of the Department of Health and Human Services.

Results and Discussion

Mechanism of the Nonresonant Femtosecond Laser Vaporization of Lipids

We first consider the nonresonant vaporization of lipids at atmospheric pressure using intense ultrafast laser pulses. Monoglyceride lipids are fatty acids that play a role in biological structure and processes in both plants and animals. The fatty acid, 1-monooleoyl-rac-glycerol or monoolein, was analyzed as a model system using LEMS. The structure of monoolein, shown as the inset in Figure 1a, contains a C18:1 unsaturated monoglyceride (where C18:1 signifies an 18 carbon chain with 1 unsaturated bond) on the hydrophobic end and two hydroxyl groups on the hydrophilic end. The nonresonant vaporization of monoolein from a steel substrate reveals the $[M+H]^+$, $[M+NH_4]^+$ and the $[M+Na]^+$ ions of monoolein at mass-to-charge (*m/z*) 357, 374, and 379, respectively, in the LEMS mass spectrum shown in Figure 1a. The ions at *m/z* 374 and 379 have been observed in literature from solutions containing ammonium acetate when performing conventional ESI-MS analysis [24]. A fragment observed at *m/z* 339 is consistent with the ion $[M–H_2O+H]^+$ and has been observed previously in atmospheric pressure chemical ionization experiments [25]. In control experiments, the low energy collision-induced dissociation (CID) did not significantly affect the $[M–H_2O+H]^+$ ion's signal intensity (data not shown). Therefore, this fragment is not the result of CID, since it is observed in both the LEMS and conventional ESI-MS experiments. Thus, we suggest that the formation of the $[M–H_2O+H]^+$ ion is due to hydrolysis.

The $[M–H_2O+H]^+$ ion was not observed when 10^{-5} M monoolein, dissolved in 1:1 (vol:vol) water:methanol with 0% acetic acid, was subjected to conventional ESI-MS (Figure 1c). As the acid concentration was increased, a monotonic increase in the $[M–H_2O+H]^+$ ion's signal intensity relative to the base peak $[M+Na]^+$ was observed (Figure 1d, e). This indicates that the use of 1% acetic acid in the electrospray solvent leads to hydrolysis of the lipid after laser vaporization. Further, when monoolein is vaporized from a metal surface into an electrospray plume composed of 1:1 (vol:vol) water:methanol containing 0% acetic acid, the $[M–H_2O+H]^+$ ion is not observed in the mass spectrum (see SP2 for mass spectrum) supporting the notion that the $[M–H_2O+H]^+$ ion is due to hydrolysis. In addition, the signal intensity for the $[M–H_2O+H]^+$ ion for

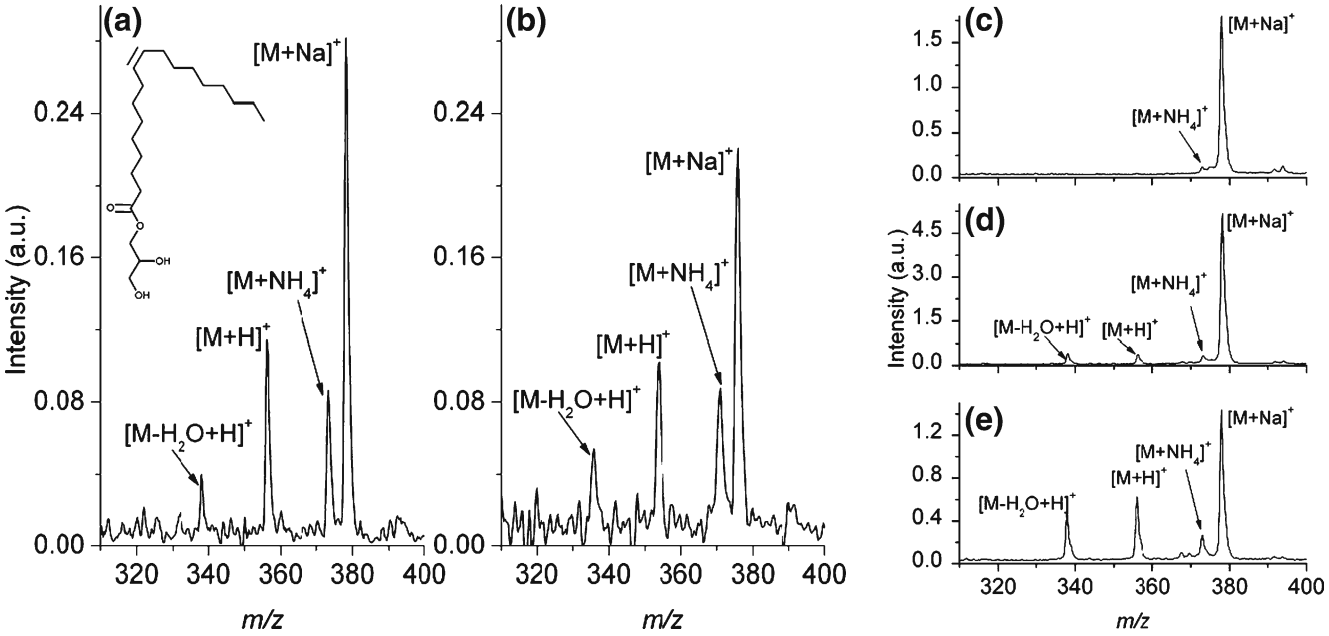

Figure 1. The background subtracted mass spectra of 1-monooleoyl-rac-glycerol (monoolein) vaporized from (**a**) metal and (**b**) glass and post-ionized in the electrospray plume. The inset in (**a**) shows the molecular structure of monoolein. The conventional ESI-MS of a 1×10^{-5} M solution of monoolein dissolved in 1:1 (vol:vol) water:methanol containing (**c**) 0%, (**d**) 0.1%, and (**e**) 1.0% acetic acid

LEMS measurements is less than the signal intensity observed in the conventional ESI mass spectral measurements (Figure 1e) under similar solvent conditions (1:1 (vol:vol) water:methanol containing 1% acetic acid). This is consistent with the short interaction time between the acidified electrospray plume and the vaporized sample (~100 ms) leading to the observed reduction in the hydrolysis fragmentation channel.

The mechanism of intense laser-induced vaporization remains an unanswered question. In the case of laser desorption using ns duration pulses, rapid heating of the substrate likely occurs, and therefore the substrate plays an important role [12]. Basic blue 7 dye was desorbed from a variety of substrates without matrix [12]. The highest signal intensity was observed when the dye was desorbed from a stainless steel surface. This is consistent with the efficient absorption of the ns laser pulse energy by the steel substrate leading to rapid heating and thermal desorption of the analyte. Femtosecond duration laser pulses can deposit energy into a molecule nonresonantly and on a timescale much faster than a thermal response, leading to the opportunity for nonthermal vaporization mechanisms. Thus, the vaporization mechanism of lipid molecules after fs laser excitation could involve excitation in the metal substrate (a strong absorber at 800 nm) or nonresonant absorption by the lipid due to the high intensity in the focused nonresonant fs laser pulse.

To address the vaporization mechanism for lipids using intense nonresonant fs laser pulses, monoolein was deposited and dried on a glass substrate. Glass is transparent at 800 nm and, therefore, no first order resonant transitions occur in that region of the electromagnetic spectrum. In addition, monoolein does not have an electronic transition in the 800 nm region, as shown in the UV/VIS absorption spectrum (see SP3 for UV/VIS absorption spectrum of monoolein). The optical penetration depth of glass at 800 nm is much greater than metal allowing the light to be transmitted through the substrate. Since there is no coupling (absorption) of the laser into the glass, there is no heating and no possibility for thermal desorption. Thus, the vaporization of monoolein deposited on a glass substrate would demonstrate the nonresonant nature of the fs vaporization process. The mass spectrum of monoolein vaporized using intense nonresonant fs laser pulses from a glass substrate is shown in Figure 1b. The $[M-H_2O+H]^+$, $[M+H]^+$, $[M+NH_4]^+$ and $[M+Na]^+$ ions are observed. Figure 1a and b show the same *m/z* peaks for the LEMS analysis of monoolein vaporized from steel and glass substrates. The signal for monoolein vaporized from a glass surface decreases in intensity presumably due to the dielectric surface undergoing patch charging. This causes a distortion of the electrospray plume, resulting in a decrease in the observed signal intensity for the laser vaporized molecules [19]. The vaporization of the lipid molecule monoolein from an insulating dielectric surface demonstrates that thermal desorption is not required for transferring molecules into the gas phase. We conclude from these experiments that a resonant transition in the substrate, sample, or matrix is not required when an intense, nonresonant fs laser is employed.

Amphiphilic molecules are the main components in biological membranes. Lipids, when placed into aqueous solution, are capable of forming bilayers and can be used to

create model membrane systems. The saturated phosphocholine lipids, DHPC and DMPC, were analyzed to investigate the nonresonant laser vaporization of precursor molecules to such model membrane systems. A 30 μL aliquot of each solution was spotted and dried on a metal slide. The molecular structure of DHPC is shown in the inset of Figure 2a and contains a C6:0 saturated diglyceride on the hydrophobic end, and a phosphate and a choline group on the hydrophilic end. The mass spectrum for DHPC vaporized from stainless steel, shown in Figure 2a, reveals the $[M+H]^+$ and $[M+Na]^+$ adduct ions at *m/z* 454 and 476, respectively. A lower abundance fragment of DHPC, consistent with the formation of the ion $[M–N(CH_3)_3+Na]^+$, was observed at *m/z* 417 and is indicated with a star in Figure 2a. This fragment ion is not observed in the control ESI-MS spectrum of DHPC (data not shown) and is presumed to be the result of nonresonant interactions with the laser. A low abundance peak observed at *m/z* 907 is consistent with the formation of the dimer ion, $[2M+H]^+$. The formation of the dimer ion of DHPC is most likely due to dipolar interactions from the polar head groups on the lipid molecules and van der Waals interactions between the nonpolar hydrocarbon tails.

The nonresonant vaporization of higher molecular weight lipids was investigated using the molecule DMPC. The mass spectrum resulting from nonresonant fs vaporization and post-ionization in an electrospray plume is shown in Figure 2b and reveals the $[M+H]^+$ and $[M+Na]^+$ ions of DMPC at *m/z* 679 and 701, respectively. The structure of the vaporized molecule, shown as the inset in Figure 2b, reveals that the hydrophobic end consists of a C14:0 saturated diglyceride and is otherwise identical to DHPC. The longer hydrocarbon tail in DMPC (leading to enhanced van der Waals interaction) in comparison to DHPC likely accounts for the higher abundance of the dimer ion detected at *m/z* 1357. This suggests that under appropriate ESI and laser conditions, the LEMS technique is capable of preserving noncovalent interactions. A fragment of DMPC was observed at *m/z* 642, indicated with an asterisk in Figure 2b, and is consistent with the formation of the ion $[M–N(CH_3)_3+Na]^+$. This low abundance fragment ion is not observed in the control ESI-MS spectrum of DMPC (data not shown) and is presumed to result from the laser vaporization process. Both the laser vaporization and dissociation processes are nonlinear and depend on the laser intensity. The degree of each process will depend on the laser intensity. Thus, the vaporization of dimer molecules does not preclude minor dissociation pathways and vice versa. We conclude that nonresonant fs laser vaporization of lipids containing phosphate and choline functional groups is possible without the need for an externally applied matrix or a first order resonant transition.

Nonresonant Femtosecond Laser Vaporization of Lipid Mixtures

To address whether the fs laser vaporization signal response is linear with concentration, we measure the mass spectra for binary mixtures of varying composition. A 30 μL aliquot of a mixture made from 10^{-4} M DHPC and 10^{-4} M monoolein was applied to a stainless steel slide. The molar ratio of DHPC: monoolein was varied between 1:0 and 0:1. The measurements shown in Figure 3 reveal a linear relationship between the amount of monoolein applied to the surface and the average integrated signal for the sum of the $[M–H_2O+H]^+$, $[M+H]^+$ and $[M+Na]^+$ ions resulting from 50 laser shots. Similarly,

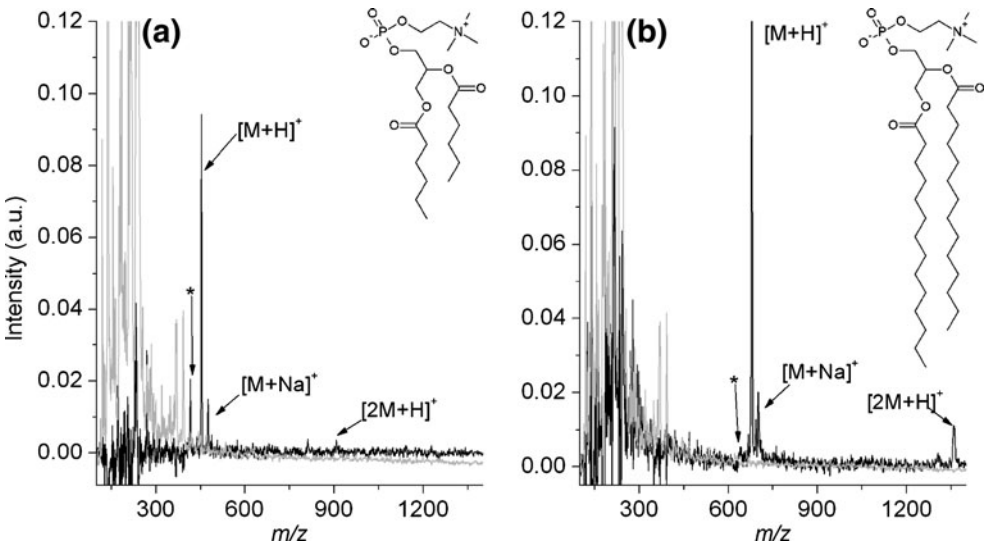

Figure 2. The background subtracted mass spectra of (**a**) DHPC and (**b**) DMPC vaporized and post-ionized in the electrospray plume. The gray lines represent the solvent background measured prior to laser vaporization and the black lines represent the background subtracted LEMS mass spectra of DHPC and DMPC. The asterisk indicates the ion $[M – N(CH_3)_3+Na]^+$ for (**a**) DHPC and (**b**) DMPC, respectively. All unlabeled peaks are solvent related

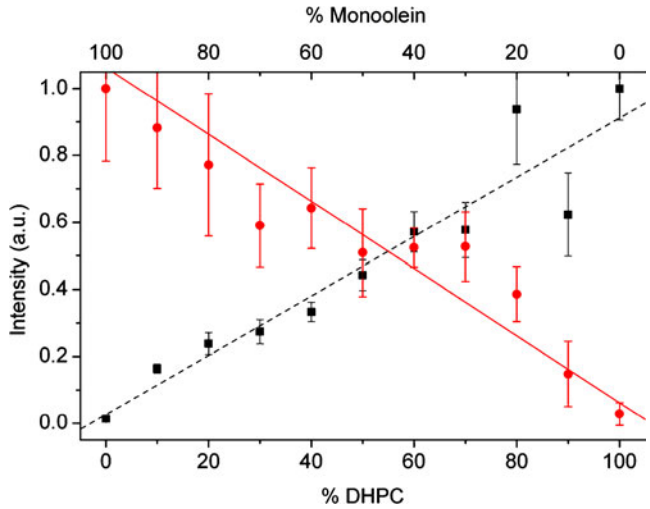

Figure 3. Plot of the average total integrated ion signal from the $[M–H_2O+H]^+$, $[M+H]^+$ and $[M+Na]^+$ ions of monoolein (filled circle ●, solid red line) and $[M+H]^+$ and $[M+Na]^+$ ions of DHPC (filled square ■, dashed black line) as a function of mixture composition

there is a linear relationship between the amount of DHPC applied to the stainless steel slide and the average integrated signal intensity for the $[M+H]^+$ and $[M+Na]^+$ ion channels. These trends suggest that the signal response in LEMS is linear with lipid concentration.

The error bars reported for the measurements in Figure 3 do not arise from fluctuations in laser intensity, or voltage fluctuations in the ESI source or mass spectrometer ion optics. The spot and dry deposition method of sample preparation yields a spatially inhomogeneous distribution of sample on the steel or glass surface. The variance is due to vaporization of an inconsistent amount of sample as a function of position on the stainless steel slide. A similar situation was observed for quantitative MALDI analysis prior to electrospray deposition of sample [26]. Nonetheless, despite the differences in size and polarity of the lipids applied to the surface, both can be detected and discriminated as a function of concentration.

LOD for the LEMS Analysis of DHPC

To determine the LOD for DHPC, a 30 μL aliquot of sample in varying concentrations was deposited onto the metal sample plate. Five averaged mass spectra could be collected per sample plate, each with an average of fifty laser shots. Therefore, approximately one-fifth of the sample is vaporized from the metal slide during the LEMS analysis. When an aliquot of 5×10^{-6} M solution of DHPC was deposited and dried on the metal surface, ~14 ng of DHPC was vaporized upon analysis. Therefore, the quantity of DHPC consumed from the sample per laser shot was < 280 pg (600 fmol). This suggests that for lipid analysis, the sensitivity per laser shot is approximately 600 fmol. It was found that the signal-to-noise for the $[M+H]^+$ ion for such a LEMS measurement was 6.3.

This is not the LOD for the nonresonant fs laser vaporization technique. The LOD of the mass spectral system depends on multiple factors including: laser parameters (wavelength, pulse duration, intensity, etc.), ionization parameters (solvent system), mass analysis technique (linear TOF, reflectron TOF, Orbitrap, etc.), amount of material deposited, film morphology and chemical noise due to interferents. By determining the quantity of sample consumed during the conventional ESI-MS analysis (~1 pg or 2.5 fmol) to the quantity consumed per laser shot for the LEMS, a better quantification of the LOD can be determined irrelevant of mass spectral system used. A comparison of the LOD for the two techniques yields that conventional ESI-MS is ~ 240× more sensitive for the analysis of DHPC. The obtained intensity curves and mass spectra for the conventional ESI-MS and LEMS analysis are shown in SP4 of the supplemental material. The decrease in sensitivity for LEMS in comparison to conventional ESI-MS is due to the neutral capture efficiency, which ranges from 2.4%±1.5% to 0.25% ±0.18% as determined from earlier LEMS experiments using pharmaceuticals [19].

Nonresonant Femtosecond Laser Vaporization of Lipids in Complex Mixtures: Blood and Milk

To investigate the detection of lipids in a complex biological mixture, a 20 μL aliquot of undiluted whole blood was spiked with 2 μL of 10^{-3} M DHPC. Lipids are typically solubilized in blood by lipoproteins, however in this experiment no proteins were added to the mixture. The LEMS mass spectrum of whole blood spiked with DHPC in an approximate 1:1 molar ratio of DHPC to hemoglobin, shown in Figure 4, reveals the $[M+H]^+$ and $[M+Na]^+$ ions of DHPC. The mass spectrum also displays the multiply charged α and β hemoglobin subunits and the α and β heme groups of the blood. The charge state distribution of the α and β hemoglobin subunit peaks is shifted to lower *m/z* with respect to a previous measurement using nonresonant fs laser vaporization [27] and is likely due to the addition of the DHPC-methanol solution. The addition of 2 μL of methanol presumably causes a portion of the α and β hemoglobin subunits to partially unfold, allowing protonation of otherwise protected basic sites. A previous investigation has also observed the α and β hemoglobin subunits from dried human blood [28] and the charge states measured are lower than those reported here. This is most likely due to the lower concentration of acetic acid in the ESI solvent. The lower concentration will cause a higher pH and will not denature the captured protein as readily as a solvent system containing 1% acetic acid.

The signal intensities of the $[M+H]^+$ and $[M+Na]^+$ ions of DHPC are lower than expected based on similar amounts of sample deposited in control experiments. This is most likely due to ion suppression from the proteins, carbohy-

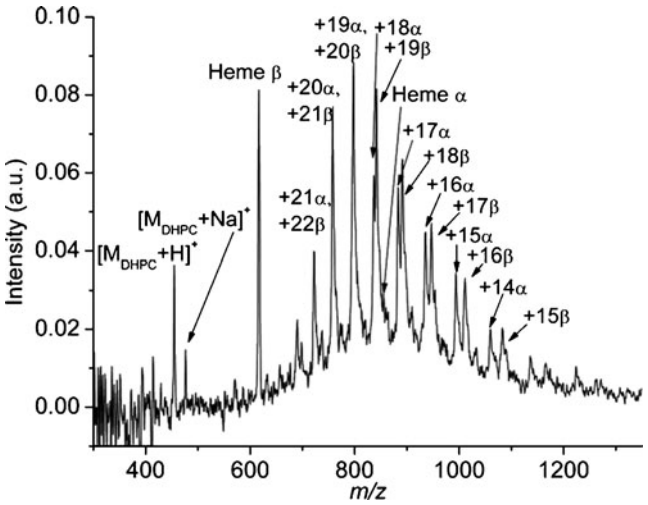

Figure 4. The background subtracted mass spectrum of laser vaporized human blood spiked with DHPC. The $[M+H]^+$ and $[M+Na]^+$ ions of DHPC can be observed along with the multiply charged α and β hemoglobin subunits and α and β heme groups of blood

drates, minerals, hormones, platelets, etc. dissolved in blood. Such ion suppression effects are common when performing post-ionization using ESI and have been observed in literature [8, 29, 30]. Despite the ion suppression effects, DHPC can still be vaporized, ionized, and analyzed from the whole blood sample. The successful detection of DHPC from undiluted whole blood suggests that other complex mixtures can be analyzed.

To determine whether LEMS is capable of directly analyzing a complex biological fluid containing a variety of polar, nonpolar and amphiphilic compounds, reduced fat and whole milk was analyzed. Milk is a liquid that is mostly composed of water but contains approximately 5% carbohydrates, 3% fat/lipid, 3% protein, and 1% vitamins and minerals by weight. The lipid content of milk usually consists of triglyceride, diacylglycerides, and phospholipids. The LEMS measurement for reduced fat milk vaporized from a welled sample plate is shown in Figure 5a. While there are a large number of distinguishing peaks detected in the milk spectrum, only 16 peaks will be discussed here. Lactose is one of the major substituents of milk composing of ~5% (wt/vol). The peaks labeled 1, 2, 4, 5, 10, 11, and 12 correspond to the lactose (mass = 342 Da) ions $[M–H_2O+H]^+$, $[M+H]^+$, $[M+Na]^+$, $[M+K]^+$, $[2M+H]^+$, $[2M+Na]^+$, $[2M+K]^+$, respectively, and are in agreement with previously reported mass spectral measurements [9, 31]. There is a broad bell shaped distribution ranging in *m/z* from 850 to 1750 in the milk mass spectrum. This distribution is similar to mass spectra obtained from the LEMS analysis of hen egg white and ovalbumin [27]. However, in milk, the distribution likely corresponds to the multiple charge states of the proteins γ-casein (mass = 24,010 Da) and α-lactoalbumin (mass = 14,175 Da). The charge state distributions for γ-casein and α-lactoalbumin were also observed by other groups that analyzed milk samples using laser-based methods [8, 32, 33]. In the mass spectrum shown in Figure 5a, the instrument parameters were adjusted to provide a mass spectrum with the highest resolution in the lower *m/z* region. When the instrument parameters were tuned for high resolution in the higher *m/z* region, the peaks for γ-casein and α-lactoalbumin were better resolved (Figure 5b).

Previous investigations performing ns laser desorption on dried whole milk [8, 34] revealed only singly charged ion peaks at *m/z* 534, 705, 724, 868, 875, 1046, and 1065. The peaks at *m/z* 705 and 724 are consistent with the $[2M+Na]^+$ and $[2M+K]^+$ ions of lactose. However, due to the lack of MS^n analysis in the previous references, the identities of the other peaks could not be determined. The lack of protein peaks in the whole milk mass spectrum was attributed to ion suppression since the lipid content of whole milk is 100 times higher than in reduced fat milk. When reduced fat milk was analyzed [8], the singly charged ions along with the charge state distributions for γ-casein and α-lactoalbumin were observed since the ion suppression effects were lower. Therefore, the singly charged peaks (at *m/z* 534, 868, 875, 1046, and 1065) were attributed to singly charged lipid ions found in milk. The peaks at *m/z* 534, 868, 875, 1046, labeled 9, 14, 15, and 16, were also observed in the LEMS mass spectrum of reduced fat milk. The peak at *m/z* 1065 [8, 34] can be observed in the high resolution LEMS spectrum, Figure 5b, but is difficult to resolve in Figure 5a. However, due to the lack of MS^n analysis in the previous references and the current investigation, the identities of these peaks were not determined.

Each of the peaks labeled 1–16 and the charge state distributions for γ-casein and α-lactoalbumin can be observed in the LEMS measurements of three different brands of reduced fat milk and whole milk (see SP5 for mass spectrum of whole milk). However, the peaks labeled 6, 7, 8, and 13 observed at *m/z* 426, 442, 501, and 783, respectively, in Figure 5 are only observed when fs lasers were used to induce vaporization, and were not detected in the ns laser desorption measurements [8, 9, 32–34]. Therefore, these peaks detected are not unique to the brand or fat content of milk analyzed but appear to be unique to the nonresonant fs vaporization of milk. The observation of carbohydrates, proteins and lipids in milk, regardless of fat content, demonstrates that LEMS is capable of analyzing complex biological fluids. In addition, the appearance of new peaks using fs vaporization with electrospray post-ionization suggests that ion suppression effects are less likely to occur despite the high concentration of interferents dissolved in the milk sample.

Laser Femtosecond Laser Vaporization of Membrane-Derived Proteins

The lipids investigated here are commonly found in the membrane of cells from living organisms. Within these membranes reside membrane-bound proteins, the detection

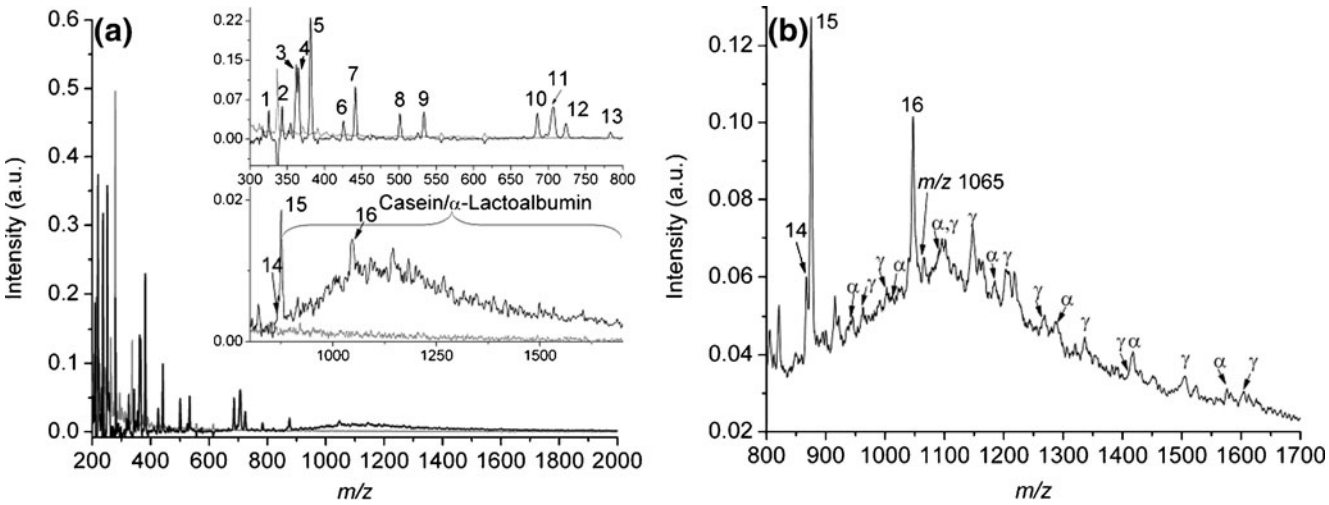

Figure 5. Peaks from lactose (1, 2, 4, 5, 10, 11, and 12), lipids (9, 13, 14, 15, and 16) and proteins γ-casein and α-lactoalbumin can be observed in the obtained background subtracted mass spectra (black line) from reduced fat milk at (**a**) low resolution and (**b**) high resolution in the high *m/z* region. The gray line represents the solvent background measured prior to laser vaporization of the milk sample

of which remains a major challenge for analytical science. Membrane-bound proteins are typically nonpolar, hydrophobic molecules making detection challenging using conventional mass spectrometric methods [35–37]. Several processing steps are required to extract hydrophobic, membrane-bound proteins for conventional ESI-MS analysis. We have demonstrated previously that nonresonant fs laser pulses coupled with electrospray post-ionization is capable of vaporizing, ionizing, and analyzing a hydrophobic porphyrin without any preprocessing steps other than deposition onto a substrate [18]. This suggests that LEMS may be capable of vaporization, ionization, and analysis of hydrophobic proteins. Here, we investigate the LEMS analysis of the hydrophobic membrane-derived proteins gramicidin A, B, and C, a class of proteins that possess antibiotic properties. In the presence of a gram positive bacterial membrane, gramicidin will insert itself into the membrane forming an ion channel. After insertion into the membrane, monocationic species residing in the bacteria's cytoplasm exit through the ion channel, eventually causing cell death [38]. Like the lipids, gramicidin A, B, and C are not soluble in water and constitute an important test for hydrophobic macromolecule analysis using LEMS.

The LEMS spectrum resulting from nonresonant fs laser vaporization of the proteins gramicidin A, B, and C deposited and dried on a steel slide is shown in Figure 6a. A broad feature corresponding to the singly charged gramicidin ions was observed at *m/z* 1882 and is consistent with the $[M_A+H]^+$ ion of gramicidin A. The resolution (m/Δm) of the linear TOF at *m/z* 2122 is ~100 and the singly charged features for gramicidin are not resolved in this *m/z* range. In the lower *m/z* region, the resolution is higher (m/Δm at *m/z* 922 ~ 120) and the mass spectral features are better resolved. The peaks observed at *m/z* 922, 930, 941.5, 952, 963, and 972 correspond to the doubly charged gramicidin $[M_B+2H]^{2+}$, $[M_C+2H]^{2+}$, $[M_A+2H]^{2+}$, $[M_C+2Na]^{2+}$, $[M_A+2Na]^{2+}$, and $[M_A+H_2O+2Na]^{2+}$ ions, respectively. The peak observed at *m/z* 1183, indicated by an asterisk, is consistent with a fragment formed via interaction with the laser pulse. The fragment at *m/z* 1183 was also observed when gramicidin was trapped in an ion cyclotron resonance cell and irradiated with a CO_2 laser pulse [39].

The conventional ESI mass spectrum of 10^{-5} M gramicidin A, B, and C in acidified 80:20 (vol:vol) methanol:water (1% glacial acetic acid) is shown in Figure 6c for comparison. A broad singly charged ion, $[M_A+H]^+$, and the doubly charged ions $[M_B+2H]^{2+}$, $[M_C+2H]^{2+}$, $[M_A+2H]^{2+}$, $[M_C+2Na]^{2+}$, $[M_A+2Na]^{2+}$, and $[M_A+H_2O+2Na]^{2+}$ were observed at *m/z* 1882, 922, 930, 941.5, 952, 963, and 972, respectively. The peak observed at *m/z* 1522 in the conventional ESI mass spectrum, indicated by a solid circle, is consistent with a fragment previously reported [39]. This ion is likely due to CID of the $[M_A+H]^+$ gramicidin A ion in the capillary exit and skimmer region. The peak observed at *m/z* 1183 in Figure 6a is attributed to laser-induced dissociation since this ion was not observed in the conventional ESI mass spectrum shown in Figure 6c. The triply charged dimer ion $[2M_A+3Na]^{3+}$ was also observed at *m/z* 1277 in Figure 6c. When the acceleration potential was increased from 140 to 380 V, the signal for the dimer ion was reduced to zero while the doubly charged ion's signal intensity increased (data not shown). The loss of the dimer ion signal can be attributed to CID between the capillary exit and skimmer region. The increase in the doubly charged ion's signal is due to the reduced amount of time the gramicidin ions spend between the capillary exit and the skimmer, causing a decrease in space charge expansion effects. This allows for a higher percentage of the ion cloud to pass through the skimmer aperture yielding a higher observed signal intensity for the doubly charged ion. Given that there are no basic or acidic sites on the molecule, we expect 1–2 charges in the folded or

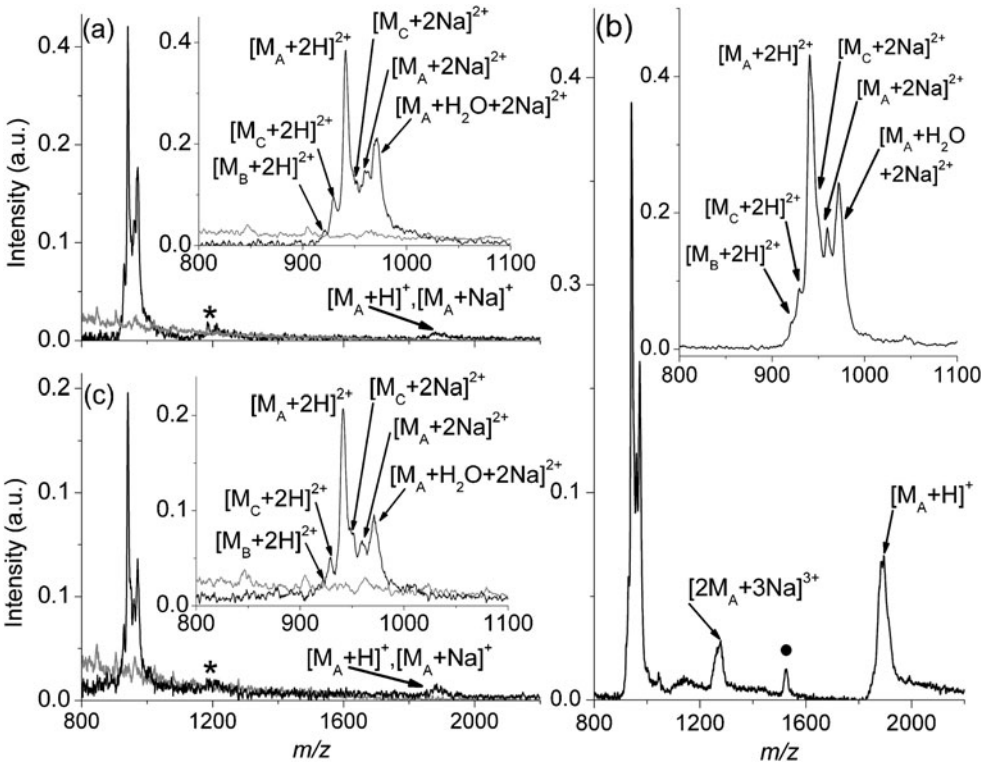

Figure 6. The background subtracted LEMS mass spectra of gramicidin A, B, and C from (**a**) a steel surface (**b**) and a glass surface. (**c**) The conventional ESI mass spectrum of a solution containing gramicidin A, B, and C. The gray line in (**a**) and (**b**) represents the solvent background measured prior to laser vaporization of the analyte. The marked peaks (asterisk *, filled circle •) denote fragments of gramicidin

unfolded state due to the terminal amino acids. These measurements demonstrate the capability of LEMS to detect hydrophobic membrane-derived proteins.

To determine whether thermal desorption or nonresonant vaporization is the underlying mechanism for hydrophobic proteins, gramicidin was deposited and dried on a glass substrate prior to fs laser vaporization. The LEMS mass spectrum of gramicidin deposited on glass, shown in Figure 6b, reveals the gramicidin A, B, and C singly and doubly charged ions along with the fragment ion at *m/z* 1183. This is similar to the spectrum of gramicidin vaporized from steel with the only difference in the spectra being that vaporization from a glass surface results in lower signal intensity and is most likely a result of patch charging. While neither glass nor gramicidin have a resonant transition in the 800 nm region and thus are transparent at this wavelength (see SP6 for UV/VIS) at low intensity, there is a higher probability for nonlinear excitation to occur in gramicidin since the lowest electronic transition in gramicidin is less than the band gap energy of the glass substrate. We note that there is no plasma generation, etching, or pitting of the glass surface after laser vaporization of the gramicidin. We conclude that the nonresonant fs pulse must couple into the gramicidin molecule to enable vaporization via a non-thermal mechanism. This indicates that a nonresonant fs laser pulse will transfer a wide range of molecules into the gas phase regardless of electronic structure, overcoming the need for resonant transitions in molecules or substrates. Nonresonant vaporization has been applied in higher intensity regimes to induce ionization as well as vaporization, but has been limited to small molecules to date [40, 41]. Nonlinear processes have also been used for a variety of techniques including stimulated emission depletion microscopy [42] and 2-photon microscopy [43], yielding enhanced spatial resolution over the traditional one photon process.

Conclusions

The universal detection of biological molecules is difficult due to the wide variety of chemical structures, polarities, and low vapor pressures for samples of interest. We have shown that LEMS is capable of detecting amphiphilic lipids and hydrophobic membrane-derived proteins from steel and glass substrates. The detection of macromolecules from a glass surface indicates that the molecules do *not* undergo thermal desorption. Once vaporized, the molecules are captured and ionized using electrospray ionization prior to mass analysis and detection using TOF mass spectrometry. Calibrated measurements demonstrate that the LEMS

method has a linear response to the components of a binary mixture of lipids. These measurements further demonstrate that the intense (10^{13} W/cm^2) nonresonant fs laser vaporization method is capable of delivering molecules, with a wide range of molecular structures and polarities, into the gas phase intact for analysis.

Acknowledgments

The authors acknowledge construction of the instrumentation supported by National Science Foundation CHE0518497. The work was supported in part by the Army Research Office W911NF0810020 and by the National Science Foundation CHE0957694. The authors thank Laine Radell and Kuriakose Simon for their help with data acquisition.

References

1. Han, X., Gross, R.W.: Quantitative Analysis and Molecular Species Fingerprinting of Triacylglyceride Molecular Species Directly from Lipid Extracts of Biological Samples by Electrospray Ionization Tandem Mass Spectrometry. *Anal. Biochem.* **1**, 88–100 (2001)
2. Petkovic, M., Schiller, J., Muller, M., Benard, S., Reichl, S., Arnold, K., Arnhold, J.: Detection of Individual Phospholipids in Lipid Mixtures by Matrix-Assisted Laser Dsorption/Ionization Time-of-Flight Mass Spectrometry: Phosphatidylcholine Prevents the Detection of Further Species. *Anal. Biochem.* **2**, 202–216 (2001)
3. Lehmann, W.D., Kessler, M.: Fatty Acid Profiling of Phospholipids by Field Desorption and Fast Atom Bombardment Mass Spectrometry. *Chem. Phys. Lipids* **2**, 123–135 (1983)
4. Ostrowski, S.G., Van Bell, C.T., Winograd, N., Ewing, A.G.: Mass Spectrometric Imaging of Highly Curved Membranes During Tetrahymena Mating. *Science* **5680**, 71–73 (2004)
5. Manicke, N.E., Wiseman, J.M., Ifa, D.R., Cooks, R.G.: Desorption Electrospray Ionization (DESI) Mass Spectrometry and Tandem Mass Spectrometry (MS/MS) of Phospholipids and Spingolipids: Ionization, Adduct Formation, and Fragmentation. *J. Am. Soc. Mass Spectrom.* **4**, 531–543 (2008)
6. Wu, C.P., Ifa, D.R., Manicke, N.E., Cooks, R.G.: Rapid, Direct Analysis of Cholesterol by Charge Labeling in Reactive Desorption Electrospray Ionization. *Anal. Chem.* **18**, 7618–7624 (2009)
7. Dill, A.L., Ifa, D.R., Manicke, N.E., Zheng, O.Y., Cooks, R.G.: Mass Spectrometric Imaging of Lipids Using Desorption Electrospray Ionization. *J. Chromatogr. B* **26**, 2883–2889 (2009)
8. Huang, M.Z., Hsu, H.J., Wu, C.I., Lin, S.Y., Ma, Y.L., Cheng, T.L., Shiea, J.: Characterization of the Chemical Components on the Surface of Different Solids with Electrospray-Assisted Laser Desorption Ionization Mass Spectrometry. *Rapid Commun. Mass Spectrom.* **11**, 1767–1775 (2007)
9. Sampson, J.S., Murray, K.K., Muddiman, D.C.: Intact and Top-Down Characterization of Biomolecules and Direct Analysis Using Infrared Matrix-Assisted Laser Desorption Electrospray Ionization Coupled to FT-ICR Mass Spectrometry. *J. Am. Soc. Mass Spectrom.* **4**, 667–673 (2009)
10. Nemes, P., Vertes, A.: Laser Ablation Electrospray Ionization for Atmospheric Pressure, In Vivo, and Imaging Mass Spectrometry. *Anal. Chem.* **21**, 8098–8106 (2007)
11. Nemes, P., Woods, A.S., Vertes, A.: Simultaneous Imaging of Small Metabolites and Lipids in Rat Brain Tissues at Atmospheric Pressure by Laser Ablation Electrospray Ionization Mass Spectrometry. *Anal. Chem.* **3**, 982–988 (2010)
12. Huang, M.-Z., Jhang, S.-S., Cheng, C.-N., Cheng, S.-C., Shiea, J.: Effects of Matrix, Electrospray Solution, and Laser Light on the Desorption and Ionization Mechanisms in Electrospray-Assisted Laser Desorption Ionization Mass Spectrometry. *Analyst* **4**, 759–766 (2010)
13. Sampson, J.S., Hawkridge, A.M., Muddiman, D.C.: Generation and Detection of Multiply-Charged Peptides and Proteins by Matrix-Assisted Laser Desorption Electrospray Ionization (MALDESI) Fourier Transform Ion Cyclotron Resonance Mass Spectrometry. *J. Am. Soc. Mass Spectrom.* **12**, 1712–1716 (2006)
14. Sampson, J.S., Hawkridge, A.M., Muddiman, D.C.: Development and Characterization of an Ionization Technique for Analysis of Biological Macromolecules: Liquid Matrix-Assisted Laser Desorption Electrospray Ionization. *Anal. Chem.* **17**, 6773–6778 (2008)
15. Chen, Z., Vertes, A.: Early Plume Expansion in Atmospheric Pressure Midinfrared Laser Ablation of Water-Rich Targets. *Phys. Rev. E* **3**, 036316 (2008)
16. Shiea, J., Huang, M.Z., Hsu, H.J., Lee, C.Y., Yuan, C.H., Beech, I., Sunner, J.: Electrospray-Assisted Laser Desorption/Ionization Mass Spectrometry for Direct Ambient Analysis of Solids. *Rapid Commun. Mass Spectrom.* **24**, 3701–3704 (2005)
17. Miziolek, A.W., Palleschi, V., Schechter, I.: Laser-Induced Breakdown Spectroscopy (LIBS) Fundamentals and Applications, p. 478. Cambridge University Press, Cambridge (2006)
18. Brady, J.J., Judge, E.J., Levis, R.J.: Mass Spectrometry of Intact Neutral Macromolecules Using Intense Non-Resonant Femtosecond Laser Vaporization with Electrospray Post-Ionization. *Rapid Commun. Mass Spectrom.* **19**, 3151–3157 (2009)
19. Judge, E.J., Brady, J.J., Levis, R.J.: Mass Analysis of Pharmaceutical Compounds from Glass, Cloth, Steel, and Wood Surfaces at Atmospheric Pressure Using Non-Resonant Femtosecond Laser Vaporization and Electrospray Ionization. *Anal. Chem.* **8**, 3231–3238 (2010)
20. Brady, J.J., Judge, E.J., Levis, R.J.: Identification of Explosives and Explosive Formulations Using Laser Electrospray Mass Spectrometry. *Rapid Commun. Mass Spectrom.* **11**, 1659–1664 (2010)
21. Bourinbaiar, A.S., Coleman, C.F.: The Effect of Gramicidin, a Topical Contraceptive and Antimicrobial Agent with Anti-HIV Activity, Against Herpes Simplex Viruses Type 1 and 2 In Vitro. *Arch. Virol.* **11**, 2225–2235 (1997)
22. Sarges, R., Witkop, B.: Gramicidin A. V. The Structure of Valine- and Isoleucine-gramicidin A. *J. Am. Chem. Soc.* **9**, 2011–2020 (1965)
23. Chitta, R.K., Gross, M.L.: Electrospray Ionization-Mass Spectrometry and Tandem Mass Spectrometry Reveal Self-Association and Metal-Ion Binding of Hydrophobic Peptides: A Study of the Gramicidin Dimer. *Biophys. J.* **1**, 473–479 (2004)
24. Eide, I., Zahlsen, K.R.: Chemical Fingerprinting of Biodiesel Using Electrospray Mass Spectrometry and Chemometrics: Characterization, Discrimination, Identification, and Quantification in Petrodiesel. *Energ. Fuel* **6**, 3702–3708 (2007)
25. Shibayama, N., Lomax, S.Q., Sutherland, K., De la Rie, E.R.: Atmospheric Pressure Chemical Ionization Liquid Chromatography Mass Spectrometry and Its Application to Conservation: Analysis of Triacylglycerols. *Stud. Conserv.* **4**, 253–268 (1999)
26. Hensel, R.R., King, R.C., Owens, K.G.: Electrospray Sample Preparation for Improved Quantitation in Matrix-Assisted Laser Desorption/Ionization Time-of-Flight Mass Spectrometry. *Rapid Commun. Mass Spectrom.* **16**, 1785–1793 (1997)
27. Judge, E.J., Brady, J.J., Levis, R.J.: Mass Analysis of Biological Macromolecules at Atmospheric Pressure Using Nonresonant Femtosecond Laser Vaporization and Electrospray Ionization. *Anal. Chem.* **24**, 10203–10207 (2010)
28. Huang, M.Z., Hsu, H.J., Lee, L.Y., Jeng, J.Y., Shiea, L.T.: Direct Protein Detection from Biological Media through Electrospray-Assisted Laser Desorption Ionization/Mass Spectrometry. *J. Proteome Res.* **5**, 1107–1116 (2006)
29. Lin, S.Y., Huang, M.Z., Chang, H.C., Shiea, J.: Using Electrospray-Assisted Laser Desorption/Ionization Mass Spectrometry to Characterize Organic Compounds Separated on Thin-Layer Chromatography Plates. *Anal. Chem.* **22**, 8789–8795 (2007)
30. Shin, Y.S., Drolet, B., Mayer, R., Dolence, K., Basile, F.: Desorption Electrospray Ionization-Mass Spectrometry of Proteins. *Anal. Chem.* **9**, 3514–3518 (2007)
31. Zhu, L., Gamez, G., Chen, H., Chingin, K., Zenobi, R.: Rapid Detection of Melamine in Untreated Milk and Wheat Gluten by Ultrasound-Assisted Extractive Electrospray Ionization Mass Spectrometry (EESI-MS). *Chem. Commun.* **5**, 559–561 (2009)
32. Shiea, J., Yuan, C.H., Huang, M.Z., Cheng, S.C., Ma, Y.L., Tseng, W.L., Chang, H.C., Hung, W.C.: Detection of Native Protein Ions in Aqueous Solution Under Ambient Conditions by Electrospray Laser Desorption/Ionization Mass Spectrometry. *Anal. Chem.* **13**, 4845–4852 (2008)
33. Cheng, S.-C., Cheng, T.-L., Chang, H.-C., Shiea, J.: Using Laser-Induced Acoustic Desorption/Electrospray Ionization Mass Spectrome-

try To Characterize Small Organic and Large Biological Compounds in the Solid State and in Solution Under Ambient Conditions. *Anal. Chem.* **3**, 868–874 (2009)
34. Jia, L., Bo, Q., Hai, L.: Fingerprinting of Yogurt Products by Laser Desorption Spray Post-Ionization Mass Spectrometry. *Rapid Commun. Mass Spectrom.* **9**, 1365–1370 (2010)
35. Mirza, S. P.; Halligan, B. D.; Greene, A. S.; Olivier, M. Improved Method for the Analysis of Membrane Proteins by Mass Spectrometry. *Physiol. Genomics* 2007**,** 89–94.
36. Wu, C.C., Yates, J.R.: The Application of Mass Spectrometry to Membrane Proteom. *Nat. Biotechnol.* **3**, 262–267 (2003)
37. Rosinke, B., Strupat, K., Hillenkamp, F., Rosenbusch, J., Dencher, N., Kruger, U., Galla, H.J.: Matrix-Assisted Laser Desorption/ Ionization Mass-Spectrometry (MALDI-MS) of Membrane-Proteins and Noncovalent Complexes. *J. Mass Spectrom.* **10**, 1462–1468 (1995)
38. Smirnov, S., Belashov, A., Demin, O.: Optimization of Antimicrobial Drug Gramicidin S Dosing Regime Using Biosimulations. *Eur. J. Pharm. Sci.* **1**, 105–109 (2009)
39. Little, D.P., Speir, J.P., Senko, M.W., O'Connor, P.B., McLafferty, F. W.: Infrared Multiphoton Dissociation of Large Multiply Charged Ions for Biomolecule Sequencing. *Anal. Chem.* **18**, 2809–2815 (1994)
40. Coello, Y., Jones, A.D., Gunaratne, T.C., Dantus, M.: Atmospheric Pressure Femtosecond Laser Imaging Mass Spectrometry. *Anal. Chem.* **7**, 2753–2758 (2010)
41. Milasinovic, S., Liu, Y.M., Gasper, G.L., Zhao, Y.B., Johnston, J.L., Gordon, R.J., Hanley, L.: Ultrashort pulse laser ablation for depth profiling of bacterial biofilms. *J. Vac. Sci. Technol. A* **4**, 647–651 (2010)
42. Moneron, G., Hell, S.W.: Two-Photon Excitation STED Microscopy. *Opt. Express* **17**, 14567–14573 (2009)
43. Denk, W., Strickler, J.H., Webb, W.W.: Two-Photon Laser Scanning Fluorescence Microscopy. *Science* **4951**, 73–76 (1990)